MORPHOLOGY AND SPATIAL DISTRIBUTION OF XUV AND X-RAY EMISSIONS IN AN ACTIVE REGION OBSERVED FROM SKYLAB

CHUNG-CHIEH CHENG, J. B. SMITH, JR.,* and E. TANDBERG-HANSSEN
NASA/Marshall Space Flight Center, Marshall Space Flight Center, Ala. 35812, U.S.A.

(Received 30 October, 1979; in revised form 4 March, 1980)

Abstract. We studied the morphology and spatial distribution of loops in an active region, using coordinated observations obtained with both the S082A XUV spectroheliograph and the S056 grazing-incidence X-ray telescope on *Skylab*. The active region loops in the temperature range 5×10^5–3×10^6 K fall basically into two distinctive groups: the hot loops with temperatures 2–3×10^6 K as observed in coronal lines and X-rays, and the relatively cool loops with temperature 5×10^5–1×10^6 K as observed in transition-zone lines (Ne VII, Mg IX). The brightest hot coronal loops in the active region are mostly low-lying, compact, closely-packed, and show greater stability than the transition-zone loops, which are fewer in number, large, and slender. The observed aspect ratio of the hot coronal loops is in the range of 0.1 and 0.2, which are almost two orders of magnitude larger than those for the Ne VII loops. Brief discussion of the MHD stability of the loops in terms of the aspect ratio is presented.

1. Introduction

Recent observations made in XUV and X-ray wavelengths have amply demonstrated that loops and arch-like structures are the dominant features in the solar corona. Visual examinations of the XUV spectroheliograms and X-ray photographs of the Sun taken with instruments on *Skylab* immediately show that active region loops with different temperatures have different gross morphology and spatial distributions of emissions. It is, however, not clear what is the precise spatial relationships between loops of widely different temperatures. In this paper we utilize coordinated observations of an active region obtained with both the S082A XUV spectroheliograph and the S056 grazing-incidence X-ray telescope on *Skylab* to study the morphology and spatial distribution of loop structures with widely separated temperatures. The temperature coverage of these observations includes the Ne VII emission at 6×10^5 K, the Fe XVI emission at 2×10^6 K, and the X-ray emission (8–16 Å) at 2–3×10^6 K. By careful co-registration of the XUV and X-ray images of the active region, we are able to determine more precisely the spatial relationship between loops of different temperatures. In addition, we identified many of the small bright emission kernels in the Ne VII and Mg IX spectroheliograms with the lower ends or footpoints of the high-temperature coronal loops in Fe XVI and X-rays. We also found, from the study of temporal behavior of loops that the stability of a loop is empirically related to its aspect ratio, a/L, where a is the radius of the loop and L its length, viz. a slender loop with small aspect ratio changes far more rapidly than a thicker loop with larger aspect ratio. Furthermore, in the active

* NOAA/Space Environment Laboratory.

Solar Physics **67** (1980) 259–265. 0038-0938/80/0672-0259$01.05.

region, high-temperature loops in Fe XVI or X-rays ($\sim 2 \times 10^6$ K) are predominately of larger aspect ratio while cooler-temperature loops in Ne VII and Mg IX are of smaller aspect ratio. In the following we first present the observational results and then the discussion.

2. Observations

The active region McMath 12379 was associated with bipolar magnetic regions. On its passage across the solar disk, the active region produced on 15 June 1973 one of the largest and best-observed flares during the *Skylab* missions. In order to avoid post-flare loops, which are by-products of the violent flaring process and thereby may be physically different from the relatively quiescent active loops, we have chosen to study the active region observed by the *Skylab* instruments on 14 June 1973, when no flare activities were reported. The XUV and X-ray instruments both had high spatial resolution approaching 2″ and observations made with them are therefore most suitable for the study of spatial distribution of coronal features. A detailed description of the XUV instrument has been given by Tousey *et al.* (1977) and of the X-ray instrument by Underwood *et al.* (1977).

Figure 1 shows the active region in Ne VII 465 Å ($T \sim 6 \times 10^5$ K), Mg IX 368 Å ($\sim 1 \times 10^6$ K), Fe XVI 335 Å ($\sim 2 \times 10^6$ K), and the X-ray emission in 8–16 Å region (~ 2–3×10^6 K), together with an Hα picture and a Kitt Peak magnetogram. The Hα picture is a positive print, while the XUV and X-ray images are negative prints. Simultaneous observations of the active region in XUV and X-rays were taken at

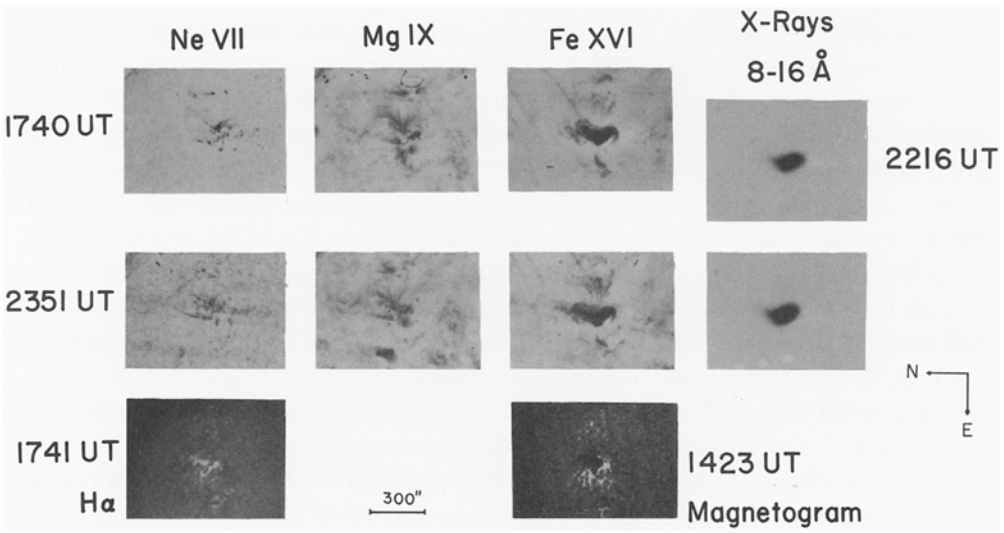

Fig. 1. Observations of the active region McMath 12379 on 14 June 1973. The XUV spectroheliograms in Ne VII 465 Å, Mg IX 368 Å and Fe XVI 335 Å, taken at 17:40 and 23:51 UT, are compared with the X-ray images, taken at 22:16 UT and 23:51 UT. Shown also are the Hα picture and the Kitt Peak magnetogram of the active region.

23:51 UT. The wide temperature span of observations shown in Figure 1 shows quite clearly the structural changes of the active region as temperature increases.

Adapting the conventional usage of chromospheric, transition zone, and coronal emission as referring to increasing temperature, it is apparent that the morphology of active region features falls into three distinctive groups. The first is the bright patches in the chromospheric emission, such as in Hα and He II. These bright patches when mapped onto the magnetograms are found to follow closely the contours of strong magnetic field regions. One bright patch is on the region with positive (white) polarity while the other is on the region with negative (black) polarity. Clearly, these patches are the loci of the footpoints of loops spanning the magnetic neutral line. No loop structures are seen in the Hα and He II emission for the active region. This is in marked contrast to the post-flare loop prominence where Hα and He II loops are prominent. The second distinct group of structural features in the active region is the Ne VII and Mg IX loops, at transition-zone temperatures. The Ne VII emission consists of few large and thin loops, and also spikes of emission which can be identified as the lower portion of an imcomplete large loop. There are also many isolated bright emission spots or kernels. When the Ne VII spectroheliograms are mapped onto the magnetograms, it is found that the footpoints of the large Ne VII loops and spikes are located mostly on the peripheries of the two magnetic regions with opposite polarity, while the Ne VII kernels fall on the strong magnetic regions on each side of the neutral line. The accuracy of the alignment between the Ne VII spectroheliogram with the magnetogram is estimated to be ±5″ or greater. In fact the Ne VII kernels follow the contour of the Hα bright patches, and are identified as the footpoints of some coronal loops as we shall see later. The large Ne VII loops connect preferably the two magnetic regions of opposite polarity farther out of the magnetic neutral line.

The morphology of the Mg IX loops is similar to that of the Ne VII loops. However, the Mg IX loops are much more diffuse and not as sharply defined as the Ne VII loops. This seems to be the general properties of Mg IX emission features in the corona. In addition to the large scale loops and spike features, the Mg IX also includes some bright diffuse kernels. The Mg IX kernels, like those in Ne VII, are seen to follow the general shape of the Hα bright emissions, and can be identified again as the lower portion of the coronal loops seen in Fe XVI and X-rays. The large loops in Mg IX have their footpoint anchored outside bright patches, as the Ne VII loops do. In order to find out if the Ne VII loops are cospatial with the Mg IX loops we have mapped the two spectroheliograms onto each other. This is simply done by moving them together along the direction of dispersion of the S082A instrument by a distance corresponding to the wavelength difference between the Ne VII and Mg IX lines. The mapping shows that, within the accuracy of ±5″ of the measurement, the general emission features in Ne VII follow the general emission features in Mg IX. Because of the differences of the Mg IX emission, many of the clearly delineated Ne VII loops have no counterparts in Mg IX emission, except that the Ne VII loops are surrounded by the diffuse Mg IX emissions.

The similarity and differences in the spatial distribution of the Ne VII and Mg IX emission can be understood in terms of their emissivity as a function of temperature. The peak of the emissivity curve of the Ne VII 465 Å line is at 6.3×10^5 K, while that of the Mg IX 368 Å line is 1×10^6 K. There is considerable overlap of the two emissivity curves in the temperature range 6×10^5 K to 1×10^6 K when both the Ne VII and Mg IX lines have strong emission. Therefore, within this temperature range, the two lines are formed at the same location where plasma of temperature 6×10^5 K exists. When the temperature increases beyond 1×10^6 K, to a value where the emissivity of the Mg IX line is 60% of its maximum value, the emissivity of the Ne VII line is reduced by more than two orders of magnitude from its peak value. The fact that the Ne VII features are sharp and the Mg IX features are diffuse indicates that Ne VII emission comes from plasmas at around 6×10^5 K while the Mg IX emission comes from plasmas with a wider range of temperature from 6×10^5 K to $\sim 1.5 \times 10^6$ K, distributed in a larger spatial extent. We notice also that there are absorption features, in the shape of a loop and a spike in the Mg IX and Ne VII emission. The absorption loop is situated side by side with the large Ne VII and Mg IX loop. These absorption features can be explained as due to He I continuum absorption at wavelength less than 504 Å. Schmahl and Orrall (1979) recently have found evidence from EUV spectra that there is considerable Lα continuum absorption at wavelength short of 912 Å in many of the EUV lines in quiet regions as well as in active regions. The presence of the He I continuum absorption features and the Ne VII loops indicate that cooler material exists high up in the active region.

The third group of structural features in the active region is the coronal loops as observed in coronal ions such as Fe XV–XVI and X-rays. The temperature of formation of these loops is in the range of $2–3 \times 10^6$ K. Figure 1 shows that the Fe XVI and X-ray emissions consist mainly of intense, compact, and closely-packed low lying loops. These loops connect the two magnetic regions with opposite polarity directly across the magnetic neutral line. As we mentioned before, the large scale Ne VII and Mg IX loops connect the two magnetic regions preferably outside of the neutral line. When the spectroheliograms of Ne VII, Mg IX, Fe XVI and X-ray image are mapped into each other, it is found that the bright kernels in Ne VII or Mg IX can be identified with the lower end or footpoint of the Fe XVI or X-ray loops. That is, the hot coronal loops are anchored on the chromospheric bright patches through the transition region which emits the Ne VII and Mg IX lines. The more or less uniform intensity distribution of X-ray and Fe XVI emission indicates that the hot loops are isothermal along most of their length, and the temperature drops sharply from coronal values to the chromospheric value. That is, there is a large temperature gradient where the Ne VII and Mg IX kernels are found.

Figure 2 shows schematically the spatial relationships between loops in Ne VII, Fe XVI, and X-rays and also their locations relative to the strong photospheric magnetic fields.

So far we have described the active region loops in terms of temperature variations. We could also characterize the transition-zone and coronal loops in terms

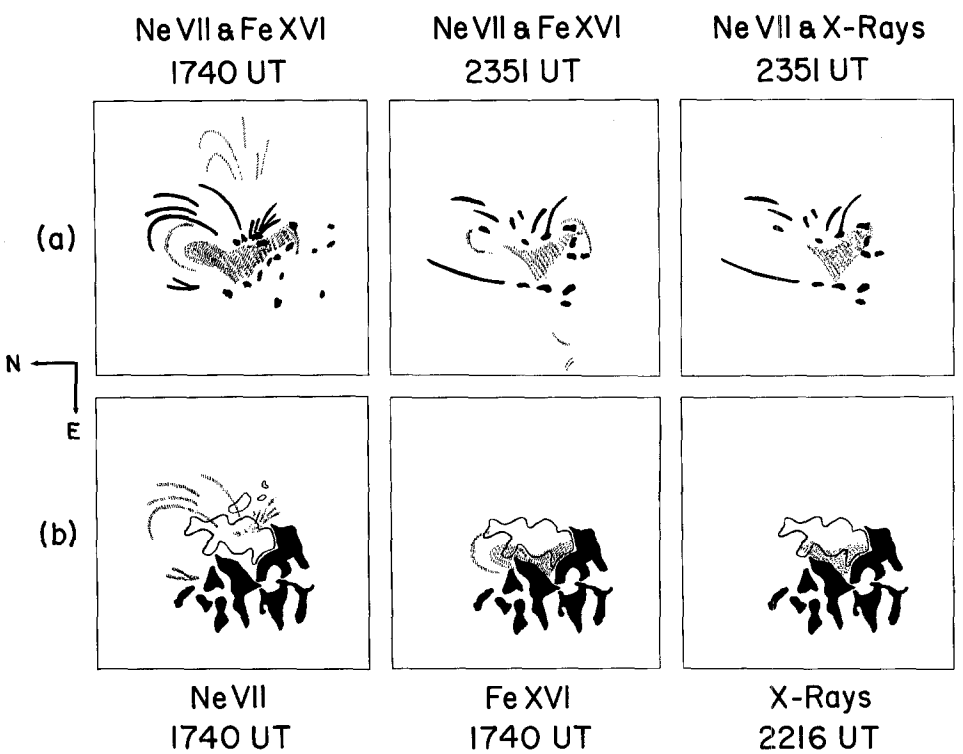

Fig. 2. (a) Comparisons of the spatial relationships of loops as observed in Ne VII, Fe XVI, and X-rays are shown schematically. The Ne VII loops are in solid black while the Fe XVI and X-ray loops are shown as shaded areas. Notice, in particular, that the bright emission kernels in Ne VII are located on each side of the Fe XVI or X-ray loops. These kernels are identified as the lower portions or footpoints of the high-temperature coronal loops. (b) The locations of the Ne VII (shaded), Fe XVI and X-ray (shaded) loops relative to regions of strong magnetic fields are shown schematically. The solid dark areas are of positive magnetic polarity and the open areas are of negative magnetic polarity.

of the aspect ratio. The length of the large Ne VII loop is about 430″ and its diameter is about 5″. This gives an aspect ratio of 6×10^{-3}, characteristic of a long and thin loop. On the other hand, the length of the intense Fe XVI and X-ray loops ranges from 40″ to 60″ while the diameter for the resolved loop is about 10 and 15″. The aspect ratio for the coronal loops is therefore in the range 0.1 and 0.2, more than one orders of magnitude larger than the Ne VII loops. In general, as the temperature increases, the aspect ratio of a loop also increases. Comparisons of observations taken many hours apart show that the active loops are remarkably stable, in the sense that their emission morphology shows very little change (Figure 1). The high temperature coronal loops in Fe XVI and X-rays are particularly stable. Comparisons of the XUV spectroheliograms and X-ray photograph of the active region McMath 12379 about 10 hr before 23:51 UT with those at 23:51 UT show that the intense compact loops vary very little, although there are changes in the larger Fe XVI loops. The Ne VII loops, on the other hand, change much more rapidly. The Ne VII loops in

the spectroheliograms taken at 17:40 UT are different from the Ne VII loops at 23:51 UT, although the overall morphology remains the same. The morphology of the chromospheric bright emission in Hα also persists for a very long time. Even during the flare of 15 June in the region, the shape of the bright patches changes very little, except that their intensity is greatly enhanced. The coronal loops which connect directly across the magnetic neutral line are more stable.

The stability is also related empirically to the aspect ratio of the loop. The Ne VII loop with its small aspect ratio shows much more variation than the Fe XVI loops with larger aspect ratio. This is also true for loops of the same temperature. As can be seen in Figure 1, the larger Fe XVI loops above the main Fe XVI loops change during this time interval of six hours when the two XUV observations are made. These loops have aspect ratio of about 0.03, about a factor of three less than the more compact intense Fe XVI and X-ray loops below. The physical significance of the aspect ratio on the stability of the loop will be discussed below.

3. Discussion

The study of the morphology and spatial distribution of the XUV and X-ray emissions in active region McMath 12379 shows that loops of various temperatures are the basic structural elements in the active region. These loops fall into two distinctive groups: the hot loops with temperature $2\text{–}3 \times 10^6$ K as observed in Fe XVI and X-rays, and the relatively cool loops with temperatures $5 \times 10^5\text{–}1 \times 10^6$ K as observed in Ne VII and Mg IX emissions. The hot coronal loops are mostly low-lying, compact, and closely-packed, while the cooler loops in Ne VII are fewer in number and are large and slender. The hot coronal loops connect directly across the neutral line separating the two magnetic regions with opposite polarity, while the cooler transition-zone loops connect the peripheries of the strong magnetic regions. The hot coronal loops do not have observable cool cores. The kind of spatial distribution of loops as observed in the McMath region 12379 seems to be the general properties of an active region.

As we have seen in the previous sections, the Ne VII loops in active region McMath 12379 which have small aspect ratio show greater variations and are less stable than the coronal loops which have, in general, larger aspect ratios. The present empirical relationship between the stability and the geometrical aspect ratio perhaps can be understood in terms of MHD theories. A plasma column with radius a and length L will be subject to MHD instabilities, for example, the kink instabilities, if the pitch of the confining magnetic field is smaller than $L/2\pi a$ (Krall and Trivelpiece, 1973). The pitch is defined as the ratio between the longitudinal and azimuthal field in the loop. Thus, for the same pitch of the confining magnetic field, a plasma column with small aspect ratio will tend to be less stable than a plasma column with larger aspect ratio. Of course, a solar loop is more complicated than the simple physical picture described here, and it is of interest to make additional studies of the time evolution of other active region loops to see if the empirical relationship between stability and the

aspect ratio is a general rule. It might turn out that this geometrically defined quantity has deeper physical significance and is an important parameter in the determination of the dynamical behavior of a loop.

At present, the physical processes leading to the formation of the cool and hot loops and their different spatial distributions are unknown and pose intriguing theoretical problems. Further quantitative studies, such as determination of the density-temperature structure in a loop, should add to our understanding of the physics involved in the seemingly simple structure of coronal loops.

Acknowledgements

One of the authors (C.C.C.) would like to thank the personnel of the Solar Terrestrial Relationships Branch at the Naval Research Laboratory for their help in carrying out the data reduction of the observations presented in this paper. Two of the authors (C.C.C. and E.T.-H.) have also benefited from their participation in the *Skylab* Solar Workshop Series on Active Regions. The Workshops are sponsored by NASA and NSF and managed by the High Altitude Observatory.

References

Krall, N. A. and Trivelpiece, A. W.: 1973, *Principle of Plasma Physics*, McGraw-Hill Book Co., New York.

Schmahl, E. J. and Orrall, F. Q.: 1979, *Astrophys. J. Letters* **231**, L41.

Tousey, R., Bartoe, J.-D. F., Brueckner, G. E., and Purcell, J. D.: 1977, *Appl. Opt.* **16**, 870.

Underwood, J. H., Milligan, J. E., deLoach, A. C., and Hoover, R. B.: 1977, *Appl. Opt.* **16**, 858.